IEEE Access
Multidisciplinary | Rapid Review | Open Access Journal

Received August 30, 2019, accepted September 16, 2019, date of publication September 19, 2019, date of current version October 2, 2019.

Digital Object Identifier 10.1109/ACCESS.2019.2942430

Low-Voltage Permittivity Control of Coplanar Lines Based on Hafnium Oxide Ferroelectrics Grown on Silicon

M. ALDRIGO, (Member, IEEE), M. DRAGOMAN, S. IORDANESCU, (Member, IEEE), F. NASTASE, S. VULPE, A. DINESCU, AND D. VASILACHE

National Institute for Research and Development in Microtechnologies, 077190 Voluntari, Romania

Corresponding author: M. Aldrigo (martino.aldrigo@imt.ro)

This work was supported by the GRAPHENEFERRO grant of UEFISCDI, under Project PN-III-P4-ID-PCCF-2016-0033.

ABSTRACT This paper is dedicated to the study of the tunable electromagnetic properties of HfO_2 doped with Zr (further referred to as HfZrO) grown on high-resistivity silicon using atomic layer deposition (ALD) techniques. Two metallic coplanar lines patterned on HfZrO having different lengths have been used to determine the effective permittivity and wave propagation constant in HfZrO in the frequency range 1-14 GHz, hence covering the L, S, C, X and (part of the) K_u bands. We have observed a significant modulation of the effective permittivity when a bias voltage is applied within the range 0-5 V, with an almost constant increase of 27% in a frequency range of 8 GHz. We have also extracted the attenuation constant, phase constant and loss tangent: the losses due to the thin HfZrO ferroelectric layer increase of maximum 21% at 5 V, which represents the saturation upper limit for ferroelectric's polarization. These results could have a significant impact on effective design of ferroelectric-based microwave circuits with tunable characteristics.

INDEX TERMS Ferroelectric films, microwave measurements, transmission lines, tunable circuits and devices.

I. INTRODUCTION

The ferroelectrics based on HfO_2 were discovered a couple of years ago by doping HfO_2 with SiO_2 [1] and with Zr [2]. It was found that the ferroelectric phase of doped HfO_2 occurs due to the formation of an orthorhombic crystalline structure. These results have triggered many researches since such ferroelectrics based on doped HfO_2 are fully CMOS-compatible. Doped HfO_2 ferroelectrics such as HfZrO have a thickness in the range 5-10 nm and very large critical electric field of 1-2 MV/cm. Thus, in deep contrast with other ferroelectrics, the doped HfO_2 ferroelectrics show a large tunability of the electrical permittivity at very low DC voltages, i.e. within the range 0-5 V. The origin of the ferroelectricity in HfO_2 should be found in the early research efforts made to increase the dielectric permittivity of HfO_2 by doping with different dopants [3]-[5], thus targeting the development of high-κ dielectrics for complementary metal-oxide-semiconductors integrated circuits. Although the orthorhombic phase is attributed to HfO_2 ferroelectricity irrespective of the doping type, a new phase of ferroelectricity was recently found [6]. The rhombohedral ferroelectric phase of HfO_2 was discovered in the last years, using epitaxial growth of HfZrO on thin films on (001)-oriented $La_{0.7}Sr_{0.3}MnO_3/SrTiO_3$. However, these substrates are not easily compatible with CMOS technologies. The interest in the development of HfO_2-based ferroelectrics and devices based on them is also illustrated by the fact that several reviews about HfO_2-based ferroelectrics have been recently published [7]–[9]. The applications of these amazing discoveries related to material science are fructified by the applications of new ferroelectrics based on doped HfO_2 in memories [9], [10], low-power transistors [11]–[13], and harvesting of electromagnetic (EM) energy based on HfZrO tunneling junctions [14]. Ferroelectrics were considered in the past the most promising materials for high-frequency tunable circuits, but this path was abandoned due to the high DC voltages required to tune the microwave circuits (i.e. in the order of tens of volts). However, it has been shown that extraordinary tunability of high-frequency devices at very

The associate editor coordinating the review of this manuscript and approving it for publication was Flavia Grassi.

low applied voltages is possible using HfZrO due to the unique physical properties of these ferroelectrics [15]. Last year, phased antenna arrays on high-resistivity silicon (HRSi) wafers based on HfZrO in the 2.5 GHz band were fabricated, conferring an unprecedented degree of miniaturization to microwave integrated circuits to be further developed by commercial companies. For example, a phase antenna array on 4-inch HfZrO/high-resistivity Si wafer working at 2.55 GHz steers its radiation beam with 25° when the applied DC bias is only ±1 V [16]. The development of further microwave applications of the HfO_2-based ferroelectrics requires the knowledge of many electromagnetic parameters such as the effective dielectric permittivity, the attenuation and phase constants, the loss tangent and their dependence on microwave frequencies and DC voltages. Therefore, we have developed an experimental procedure to find them in the case of HfZrO which is the most used ferroelectric based on HfO_2 doped with Zr.

II. FABRICATION AND CHARACTERIZATION OF COPLANAR LINES ON HAFNIUM OXIDE FERROELECTRIC ON SILICON

Classical methods used to characterize multilayer CPWs, such as single layer reduction (SLR) technique [17] or microstrip dual resonator [18], fail due to the extremely low thickness of the HfZrO ferroelectric layer, so that the relative permittivity at microwaves can be extracted only via a fitting procedure using EM simulations. However, for engineering applications, the effective permittivity is a more useful reference to design radiofrequency devices. Therefore, for the purpose of this work we performed a batch fabrication of HfZrO with a thickness of 6 nm on HRSi (Float-Zone Hyper Pure Silicon (FZ-HPS) P(100) by Topsil, resistivity $\rho > 10,000\Omega$·cm), with thickness of 525 μm using ALD growth methods and we used a series of characterization techniques to assign ferroelectricity to HfZrO. The details of fabrication and characterization (using PFM, XRD and XPS) are presented in [10] and in the Appendix. It is worth mentioning here two main aspects: (i) prior to the ALD process, the silicon wafer was subjected to surface treatment by exposure to UV-ozone for 15 min. at 75°C; this guarantees the enhance of wettability and surface free energy, which play an important role for the initial growth and nucleation of the thin film in the ALD process; (ii) the deposition was done with 60 ALD cycles at 200°C, the film thickness being confirmed by X-ray reflectivity (XRR) to be 6.2 nm (average value). Electron beam metallization technique was used to deposit metallic coplanar lines on HRSi. In this way, tens of coplanar waveguide lines (CPW) with two different lengths were fabricated on HfZrO grown on HRSi.

The metallization of CPWs is 50 nm/500 nm-thick Ti/Au layer, the width of the CPWs is W=1 mm, while their lengths are $L_A = 6.671$ mm and $L_B = 2.393$ mm, respectively. An example of such HfZrO CPW line is given in Fig. 1.

It has to be pointed out that the experimental determination of the effective dielectric permittivity and propagation

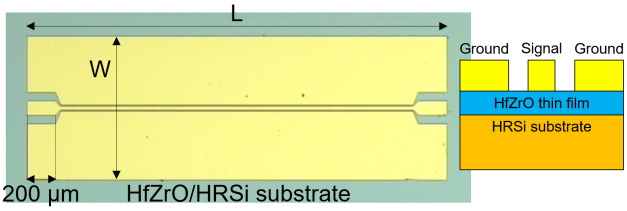

FIGURE 1. Optical image of the HfZrO/HRSi-based CPW (top-view, L=L_A or L=L_B) with a schematic of the cross-section (right).

constants of a material with a thickness of only 6 nm, which is orders of magnitude lower than the wavelengths in microwave spectrum, is not a simple task. Therefore, we used narrow CPWs (10 μm gap width and 25 μm signal line width) where the propagation of the electromagnetic field is better confined at the interface between metal and HRSi bulk substrate or, in other words, inside the ferroelectric film (thus reducing both dielectric and radiation losses). We also tried to perform THz ellipsometry tests on HRSi/HfZrO samples of 1 cm × 1 cm: due to the extremely low thickness of the ferroelectric layer, the measurement sensibility was not high enough to distinguish between ferroelectric's and silicon's permittivity.

In detail, the DC bias voltage is applied between CPW signal line and CPW lateral ground and the associated electric field (of maximum 5 kV/cm) has a predominant in-plane component due to the small gap value. This can be seen in Fig. 2, where the simulated electrostatic field is presented for three cases: (a) CPW gap-signal-gap-configuration of 10/25/10 μm on HfZrO/HRSi; (b) CPW gap-signal-gap-configuration of 60/100/60 μm on HfZrO/HRSi; (c) CPW gap-signal-gap-configuration of 10/25/10 μm on HRSi. The 60/100/60 μm is largely used as reference geometry for standard CPW probe tips with 150 μm-pitch. The simulations have been carried out by imposing a 0 V potential on the lateral ground planes and a 1 V potential on the signal line. They provide an accurate overview of how the static electric field (E-field) is distributed in the structure, comprehensive of the interfaces between adjacent layers.

From Figs. 2a and 2b it can be noticed that there is a strong concentration of static E-field in the CPW gaps, confined inside the HfZrO layer. This is confirmed by the values of the computed E-field energy, shown in Table I: the energy in the HRSi substrate is almost the same, whereas the energy in the HfZrO layer is one order of magnitude higher for the CPW with gap of 10 μm, thus giving a clear proof of the advantage in choosing such a configuration to better confine the effect of a DC bias into the thin HfZrO ferroelectric. In Fig. 2c, one can notice that, in absence of the HfZrO thin film, the static E-field in the bulk substrate is still very low, with an overall increase of the corresponding energy of just 21% with respect to the case of Fig. 2a, as can be seen in Table I. This means that the energy accumulated in the HfZrO layer is stored at the fringing edges of CPW's metallization when the HfZrO is absent.

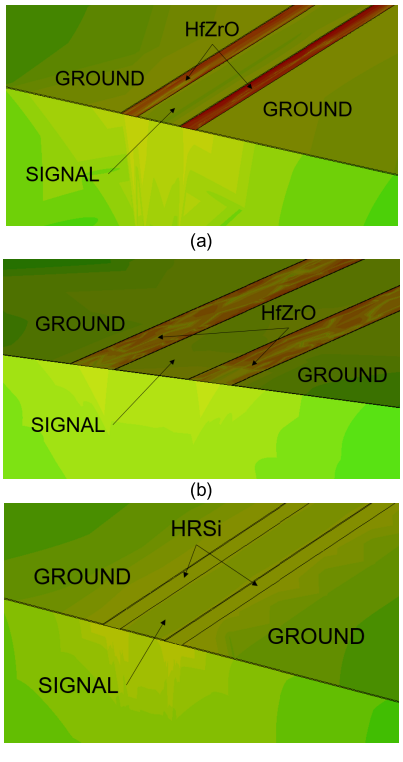

FIGURE 2. Simulated distribution of the static E-field in the CPW line (a) on HfZrO/HRSi with gap of 10μm; (b) on HfZrO/HRSi with gap of 60μm; (c) on HRSi with gap of 10 μm.

TABLE 1. Simulated static electric field energy.

CPW dimensions	Energy in HRSi (J)	Energy in HfZrO (J)
10/25/10 µm	5.28×10^{-13}	1.28×10^{-9}
60/100/60 µm	5.29×10^{-13}	1.7×10^{-10}
10/25/10 µm on HRSi	6.39×10^{-13}	–

The propagation constant within the CPW structures is given by:

$$\gamma = \alpha + j\beta = \alpha + j2\pi f\sqrt{\varepsilon_{eff}}/c_0 \quad (1)$$

where α is the attenuation constant, β is the phase constant, ε_{eff} is the effective permittivity and c_0 is the speed of light in vacuum. The propagation constant can be extracted from the measured S-parameters of the CPW lines having the lengths L_A and L_B, using the following Bianco-Parodi formula [19]:

$$\gamma = cosh^{-1}\left[(\Delta S - \Delta_A - \Delta_B)\Big/\left(2S_{21}^A S_{21}^B\right)\right]\Big/\Delta L \quad (2)$$

$$\Delta S = S_{11}^B S_{22}^A + S_{11}^A S_{22}^B \quad (2a)$$

$$\Delta_{A(B)} = S_{11}^{A(B)} S_{22}^{A(B)} - S_{12}^{A(B)} S_{21}^{A(B)} \quad (2b)$$

$$\Delta L = |L_A - L_B| \quad (2c)$$

where $|L_A - L_B| = 3.732$ mm. We stress here that the selected frequency range (1-14 GHz) provides results in a band of practical interest for engineering applications at microwaves; furthermore, it is consistent with previous results regarding the exploitation of ferroelectric properties of HfZrO in a band where the ferroelectricity has a maximum impact upon device's performance [16].

III. MICROWAVE MEASUREMENTS OF COPLANAR LINES ON HAFNIUM OXIDE FERROELECTRIC ON SILICON: ELECTRICAL TUNABILITY AND PARAMETER EXTRACTION

We have measured the scattering parameters, i.e. reflection (S_{11} and S_{22}) and transmission (S_{21} and S_{12}) parameters of tens of CPWs on HRSi and on HfZrO/HRSi to distinguish between the electromagnetic propagation contributions of the sole HRSi and of the HfZrO/HRSi substrate, the relative error when measuring the S-parameters of all samples being less than 0.5%. The measurements have been made at room temperature in dark conditions (to avoid any interference from undesired light sources), directly on-wafer with a vector network analyzer (VNA) Anritsu-37397D connected to a Karl-Süss PM5 probe station, the DC polarization being made using the internal bias tees of the VNA. The VNA has been calibrated via standard short-open-load-thru (SOLT) technique before measurements (with a calibration kit guaranteed by NIST), the reference plane being in correspondence of the two 200 μm-long input/output launching lines for connection to the probe tips (shown in Fig. 1). All CPW configurations (i.e. 60/100/60 μm at input/output ports, short tapered sections, and 10/25/10 μm) are designed and simulated to keep the same reference characteristic impedance around 50 Ω, so that geometry discontinuities do not reflect into impedance mismatch. This means that the expected error in the extraction of the effective permittivity through Eqs. (2)-(2c) is less than 1%, and it is due solely to the different gap's width at input/output ports (as demonstrated in Section II, Fig. 2, this width causes a reduction of the E-field strength in the HfZrO layer when increasing the gap).

The measured modulus (dB scale) of the S-parameters for the two lines of length L_A and L_B, as a function of frequency and positive applied DC bias, are displayed in Figs. 3a and 3b, respectively. It is apparent that, for both reflection and transmission parameters, the curves related to the two cases – CPW on HRSi (black solid/dotted lines) and CPW on HfZrO on HRSi at 0 V (pink lines) – are very similar: this result is supported by the fact that the HfZrO layer is very thin (the aspect ratio with respect to the HRSi substrate is 1:84,677) and, in absence of an applied DC bias, its influence on the overall electrical characteristics of the CPW line is reduced. One can also notice two aspects: (i) the reflection parameter (S_{11}) is always better than −15 dB, which means that the CPW lines of length L_A and L_B are well matched to 50 Ω, since

$$S_{ik} = (V_i - I_i Z_c)\Big/(V_k - I_k Z_c) \quad (3)$$

where Z_c is the reference characteristic impedance (50 Ω), while $V_{i,k}$ and $I_{i,k}$ are the voltage and current modelling the CPW line and taking into account the DC bias effect on the HfZrO thin film; (ii) up to about 2.5 GHz, the transmission parameter (S_{21}) of the CPW on HfZrO/HRSi at 0 V and 2 V

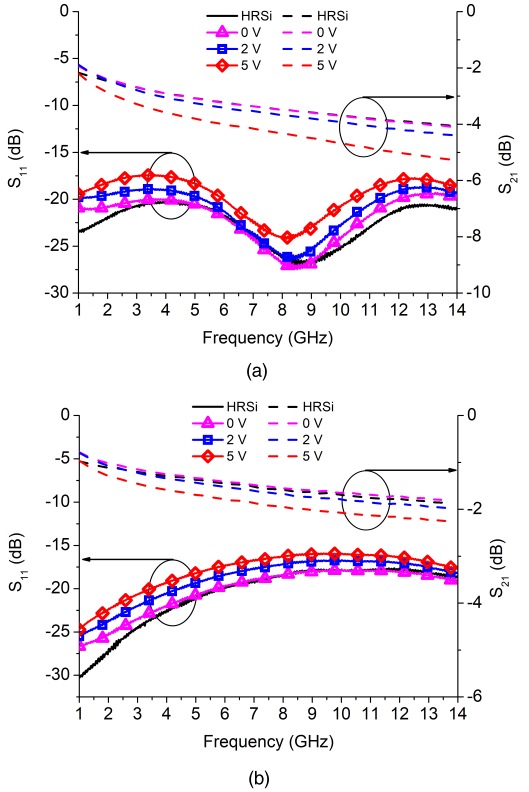

FIGURE 3. Measured modulus (dB scale) of S-parameters (reflection parameter – S_{11} – and transmission parameter – S_{21}) of the CPW lines of length (a) L_A and (b) L_B, as a function of frequency and applied positive DC bias.

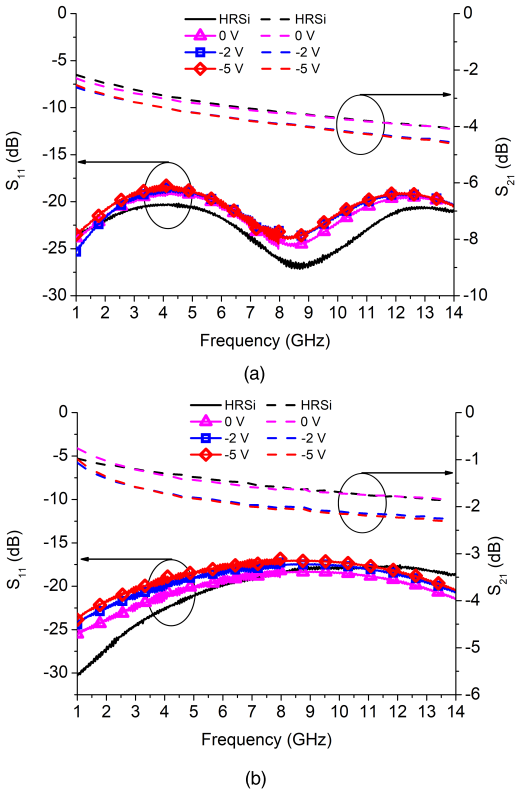

FIGURE 4. Measured modulus (dB scale) of S-parameters (reflection parameter – S_{11} – and transmission parameter – S_{21}) of the CPW lines of length (a) L_A and (b) L_B, as a function of frequency and applied negative DC bias.

DC bias is better than the transmission of the CPW on HRSi, even if this difference is very low: just 0.24 dB at 1 GHz for the CPW line of length L_A, and just 0.19 dB at 1 GHz for the CPW line of length L_B. In this respect, a possible explanation could be found in the complex frequency-dependent energy-loss behavior in ferroelectrics, together with a change in HfZrO's permittivity and attenuation/phase constants under an external DC bias. Moreover, all measured results are normalized to Z_c.

We have noticed that the most significant results for CPW lines in terms of variation of their electrical characteristics can be obtained for positive DC bias values. The proof is given by the measured scattering parameters for negative DC bias values, shown in Figs. 4a and 4b: with respect to the homologous results displayed in Figs. 3a and 3b, it is evident the clearly present but less pronounced ferroelectric effect when biasing the CPW lines with -2 V and -5 V. The explanation for this phenomenon can be found in the built-in field which forms at the HRSi/HfZrO interface [20]: it is well known that this field induces an asymmetry in the ferroelectric hysteresis loop and, together with the external DC electric field, affects both ferroelectric double well potential and polarization states.

The effective permittivity is displayed in Fig. 5, in two cases: HRSi and HfZrO on Si (in this case, at three values of the applied DC voltage, i.e. 0 V, 2 V and 5 V). We set the upper DC bias value to 5 V since this is a saturation limit, beyond which no significant changes can be observed in the measured parameters. It has to be pointed out that the effective permittivity is the relevant parameter for high frequency CPWs since it takes into account the substrate, its losses and the geometry of CPW. First, we have measured the S-parameters and have extracted the effective permittivity of CPWs patterned directly of HRSi, using Eqs. (1) and (2). Then, we have measured the S-parameters of the CPW patterned on the HfZrO grown on HRSi. Both CPW lines have the same dimensions and the same metallization. In the case of CPW patterned directly on HRSi there is no variation of effective permittivity with applied DC bias (as expected), while in the case of CPW patterned on HfZrO, it can be seen that ε_{eff} is shifted upward with the applied voltage, which is the clear proof of ferroelectricity in HfZrO (since ferroelectrics are the only materials able to change their permittivity with an applied DC voltage [21]). There is a significant change in the effective electrical permittivity with DC bias: at 2.45 GHz the effective permittivity is 7.61 at 0 V and 9.64 at 5 V, so a change of 27% is produced, while at 10 GHz $\varepsilon_{eff} = 6.79$ at 0 V and $\varepsilon_{eff} = 7.89$ at 5 V, so an almost constant increase of 27% is obtained in the frequency range 2-10 GHz when the CPW patterned on HfZrO on HRSi is biased at 5 V. It can be also observed that in the

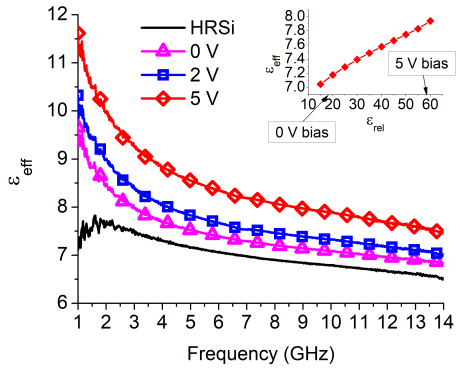

FIGURE 5. Effective permittivity dependence on frequency and DC bias extracted from experimental data for HRSi and HfZrO on HRSi at 0 V, 2 V and 5 V DC bias. Inset: Effective permittivity vs. relative permittivity, as obtained by an EM simulation fitting procedure at 10 GHz.

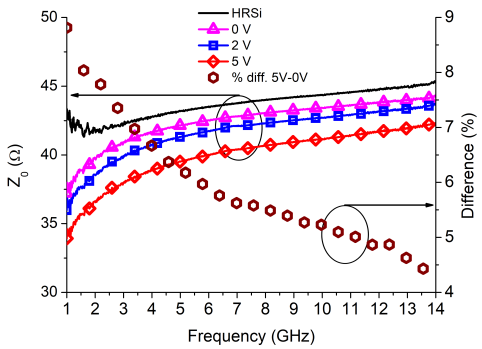

FIGURE 6. Extracted characteristic impedance as a function of frequency and DC bias (left axis). On the right axis, the percentage difference between the case 5 V and 0 V is displayed, showing the variation of Z_0 due to biasing of the HfZrO thin film.

same frequency range, when a DC bias of 2 V is applied the increase of the effective permittivity is 16%. The inset in Fig. 5 shows the extracted effective permittivity at 10 GHz as a function of the relative permittivity (ε_{rel}), as obtained by a fitting procedure in CST MW Studio®: the values of ε_{rel} are in good agreement with previous experiments [22], showing how it spans the range 18–58 when applying a bias of maximum 5 V. This result is a proof of the utility of the chosen geometry strictly for characterizing the HfZrO layer at high frequencies. The choice of a particular CPW geometry was necessary to better observe the effect of biasing on the HfZrO layer. However, the extracted values of ε_{eff} (which depends on the geometry itself) can be used to estimate the relative permittivity, which does not depend on geometry, thus giving important information about the electrical properties of HfZrO ferroelectric thin films at microwaves.

Even if the proposed device can be classified as a metal-oxide-semiconductor (MOS) structure, there are two main differences: (i) a typical MOS structure entails a p- or n-type doped semiconductor substrate [23] (whereas we have used high-resistivity silicon). In [24], even if an undoped semiconductor is deployed, an oxide with thickness of tens of nm exclusively provides a change in the attenuation constant due to additional losses caused by interface charges, i.e. no effective tuning phenomena are reported for the phase constant; (ii) from our experiments (also carried out on HfZrO-based interdigitated (IDT) varactors and antenna arrays [15], [16], [25]), no varactor-like effect can be observed when applying a DC bias on the test devices fabricated on HRSi. It has to be stressed here that the benchmark case of CPW lines on HRSi refers to the case of components with the gold metallization deposited directly on HRSi, on which only a native 1.5 nm-thick oxide layer of SiO_2 is likely present if exposed to air. Therefore, the influence of this native oxide on the overall performance of the CPW lines is negligible and, hence, does not imply any modulation of the scattering parameters when applying a DC bias. In other words, the low-voltage control of all the electrical parameters of the CPW lines is due solely to the presence of the 6 nm-thick HfZrO layer, which allows tuning both attenuation and phase constants, the latter being the specific mark given by a ferroelectric material, whereas the HRSi semiconductor does not have its carrier concentration modulated with the applied bias. Furthermore, a conventional MOS structure is (in general) a vertical stack made of a metal top gate, an oxide layer, a semiconductor and a metal contact to the back of the semiconductor, whereas we have designed CPW lines, hence planar (horizontal) devices, which means a different physical mechanism when applying a DC bias between signal and ground. Since the aim of this work is to offer an exhaustive DC/microwave characterization of high-frequency coplanar lines for CMOS-compatible circuits integrated with low-voltage tunable Hf-based ferroelectrics, in order to further verify the ferroelectric nature of such compounds we have also tested IDT capacitors (of the same type described in [25]), fabricated on the same HRSi wafer together with the proposed CPW lines: they show a phase shifter-like behavior for both positive and negative DC bias values. For a conventional CPW on a dielectric substrate of finite thickness, its characteristic impedance Z_0 can be computed as follows [26]:

$$Z_0 = 30\pi \Big/ \sqrt{\varepsilon_{eff}} K\left(k_0'\right) \Big/ K\left(k_0\right) \tag{4a}$$

$$k_0 = S \Big/ \left(S + 2W\right) \tag{4b}$$

where $K(\bullet)$ is the complete elliptic integral, S is the width of the signal line and W is the width of the gap of the CPW. In the present case of study, the computation is not rigorous due to the presence of the thin HfZrO layer; however, an approximate estimation provides a variation of Z_0 (see Fig. 6) over the band of interest in the range 4.45%–8.83% between the two cases of 0 V and 5 V DC bias.

From Fig. 6, one can notice that Z_0 is almost constant over the band of interest for the case of HRSi, whereas it varies significantly in frequency as the applied bias increases from 0 V up to 5 V. For example, the value of Z_0 at 1 GHz is (for the CPW lines on HRSi) 43.33 Ω, and (for the CPW lines on HfZrO/HRSi) 37.31 Ω at 0 V bias and 34.02 Ω at 5 V bias. In other words, Z_0 varies between 14% and 21% due to the presence of the ferroelectric thin layer when

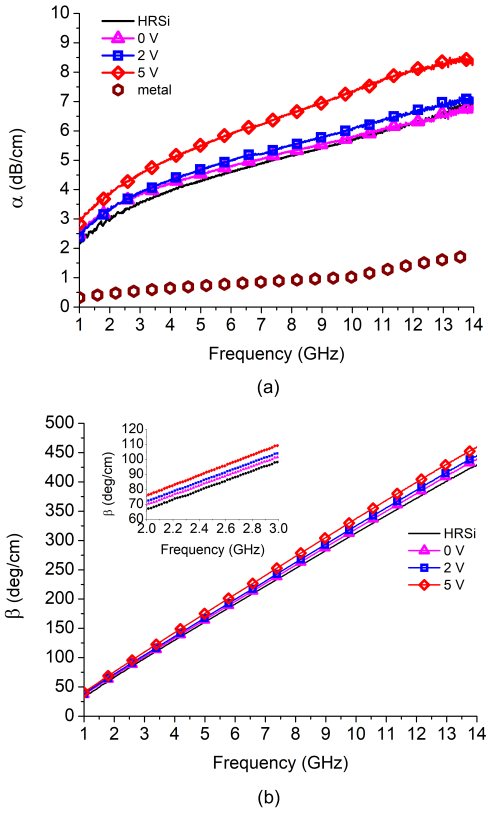

FIGURE 7. (a) Attenuation and (b) phase constant (inset: Magnification in the band 2-3 GHz) as a function of frequency and DC bias.

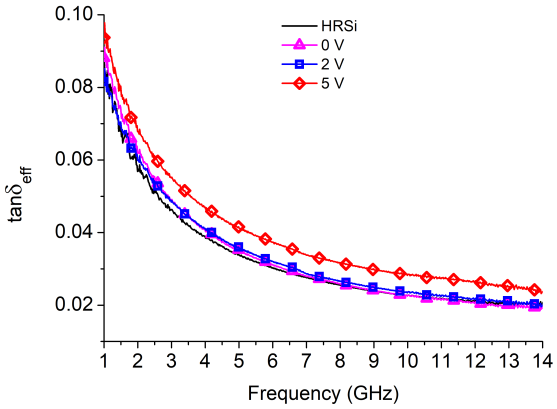

FIGURE 8. Effective loss tangent as a function of frequency and DC bias.

comparing to a CPW on HRSi. We have also extracted from the measured S-parameters both α and β and the effective loss tangent ($\tan\delta_{eff}$) at various DC voltages, the results being represented in Fig. 7 and Fig. 8, respectively. One can see that the attenuation constant α varies in the range 2-10 dB/cm, while the phase constant β changes within 30-500 deg/cm. For the sake of completeness, we also show the extracted attenuation due to the gold metallization (''metal'' in Fig. 7a). Both constants increase with the value of the applied voltage, as this phenomenon is related to an increase of CPW's reactance or, in other words, a decrease of the capacitance provided by the HfZrO thin layer. This way, the electromagnetic waves propagate in the HfZrO/HRSi substrate with rather low attenuation while the phase shift is controlled by the DC bias. There is a difference in phase of 10°/cm when biasing the HfZrO-based CPW from 0 V up to 5 V. Finally, the calculated effective loss tangent at 5 V is 0.06 at 2.45 GHz, 0.04 at 5.8 GHz, and 0.03 at 10 GHz. These results demonstrate that the effective losses are reasonably low in the considered frequency range and show small variations with the applied DC voltage. Furthermore, the chosen thickness for the HfZrO layer (i.e. 6.2 nm) is the optimum for maximizing the ferroelectric properties of such material, as already demonstrated [14]–[16], [25]. Thicker films (up to 10 nm) exhibit weaker ferroelectric characteristics and, above that value, HfZrO tends to become a pure dielectric. As regards the particular CPW configuration used in this work, as shown in Section II it represents a good solution to test the permittivity control of planar guiding structures, another useful test structure being represented by planar phase shifters, in which the small distance between adjacent digits enhances the overall capacitive effect [15], [16], [25]. IDT capacitors [16], [25] on ferroelectric HfO_2-based thin films deposited via selective ALD will be the targeted solution for future microwave applications employing ferroelectric varactors, in order to avoid the exploitation of long CPW lines on HfZrO/HRSi. In detail, selective ALD allows depositing the ferroelectric layer only in the area of interest for the design of the phase shifters embedded in the structure, thus limiting microwave losses.

As regards a possible dependence of the performance of the HfZrO ferroelectric on temperature, a very recent paper [27] clearly demonstrates how the ferroelectric physical properties of HfZrO thin films exhibit very little variations over a broad temperature range (i.e. 100 K–450 K), hence proving that HfZrO is a temperature-stable ferroelectric. We also carried out extensive experiments on HfZrO-based IDT phase shifters, from which we observed a good stability of the ferroelectric phase of 6-10 nm-thick HfZrO layers up to about 140°C, thus confirming the results in [27] (these results will be reported elsewhere).

IV. CONCLUSION

In this paper, the electromagnetic propagation parameters of a CPW based on HfZrO/HRSi have been experimentally determined showing that the effective permittivity of the CPW waveguide is increasing with 27% when a DC bias of maximum 5 V is applied. This fact has important consequences on reconfigurable circuits which are CMOS-compatible and operate at very high frequencies.

APPENDIX: FABRICATION AND PHYSICAL CHARACTERIZATION OF FERROELECTRIC THIN FILMS

An Oxford Instruments OpAL ALD reactor was used for manufacturing of ferroelectric thin films using Tetrakis (dimethylamino)hafnium (TDMAH, 99.99+%-Hf, <0.2%-Zr, Puratrem, USA) and Tetrakis(dimethylamino)zirconium(IV) (TDMAZ, 99.99%-Zr, Puratrem, USA) as metal

organic precursors. Ultra-pure water was used as the oxidant, and ultra-high purity nitrogen (Nitrogen 6.0, 99.9999 vol. %) was used as the purge and carrier gas. Zirconium-doped HfO_2 thin films were deposited on a 4-inch high-resistivity Si wafer (HRSi, with thickness of 525 μm). Prior to the ALD process, the silicon wafer was subjected to surface cleaner treatment by exposure to UV-ozone for 15 minutes at 75°C, using an UV-Ozone cleaner (Novascan Technologies, USA). To obtain zirconium-doped HfO_2 thin films with a Zr content as homogeneously distributed, the ferroelectric thin films were deposited by mixing the two organometallic precursors into the ALD reactor chamber. For the growth of $Hf_xZr_{1-x}O_2$ (HfZrO) films the two organometallic precursors were pulsed simultaneously in a 1:1 ratio followed by the ALD purging and oxidation steps. Considering the fact that the growth rate of pure HfO_2 and pure ZrO_2 are both ∼0.1 nm per cycle at 200°C, and both organometallic precursors have a similar chemical structure, it is expected that the growth rate for HfZrO to be approximately the same. The deposition was done with 60 ALD cycles (around 6 nm) at 200°C. The film thickness was confirmed by X-ray reflectivity (period of the Kiessig fringes) to be 6.2 nm. XRR and grazing incidence X-ray diffraction (GIXRD) measurements were performed using a high-resolution X-ray diffractometer (Rigaku SmartLab) that employs CuKα1 radiation ($\lambda = 1.54$ Å). The incidence angle was set to 0.35°. In addition, XRR measurements were used to calculate the density of thin films. XRR measurements found the layer density at 9.15 g/cm^3, very close to the bulk density of HfO_2 (i.e. 9.68 g/cm^3). Fig. 9 shows the GIXRD spectra of the HfZrO film in the wide 2θ range of 20-70°, and indicates the coexistence of multiple phases within the zirconium doped HfO_2 thin films. The most intense diffraction peak is formed by the presence of overlapping reflections associated to the tetragonal ($P4_2$/nmc) and the non-centrosymmetric orthorhombic phase ($Pbc2_1$). Because the parameters of their lattice are almost identical, the GIXRD measurement cannot clearly distinguish the orthorhombic and tetragonal structures of HfO_2 [28]. Through a suitable combination of stress and/or electric field, the tetragonal $P4_2$/nmc phase may switch into the polar orthorhombic $Pbc2_1$ phase [29]. The formation of the orthorhombic phase in zirconium doped HfO_2 thin films, with $Pbc2_1$ symmetry, is confirmed by the presence of the two diffraction peaks near $2\theta = 30.5°$ and 55° assigned to $(111)_o$ and $(220)_o$ reflections [2]. The absence of the monoclinic (-111) reflections (expected around 28° at 2θ angle) and the presence of the (111) and (011) reflections of the orthorhombic and tetragonal phases, indicate that the film has a polycrystalline structure in which the ferroelectric phase is dominant. The sharp reflections in the GIXRD which appear around 51°-53° are attributed to the signal from the Si substrate.

The surface morphology and roughness of the zirconium doped HfO_2 thin films were examined by atomic force microscopy (AFM) on a "NTEGRA Aura" Scanning Probe Microscope device designed by NT-MDT company. All AFM images were acquired in intermittent-contact mode, using high accuracy noncontact (HA_NC, NT-MDT) silicon probes with less than 10 nm nominal tip radius. Roughness analysis was performed using the NT-MDT Nova^{TM}software. For roughness calculations, scanning areas of 2 μm×2 μm were used. AFM image displayed in Fig. 10 reveal continuous and homogeneous surface morphologies without pin-holes, and RMS roughness values lie below 0.2 nm (RMS∼0.18 nm). The very smooth surface texture and very low roughness of the ultra-thin films provides the first information about their composition and structure, which are relatively constant in volume [30].

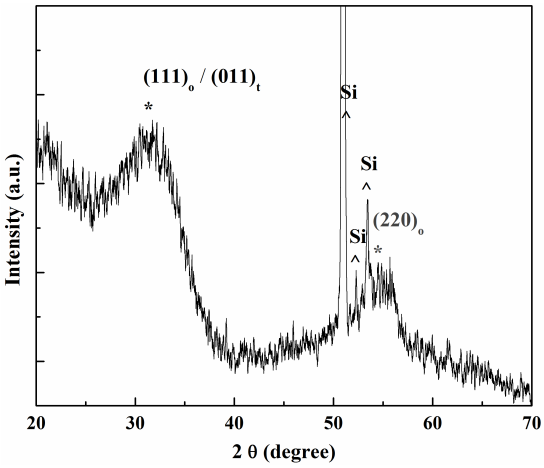

FIGURE 9. Grazing incidence X-ray diffraction (GIXRD) spectra of the ∼6 nm-thick HfZrO thin film.

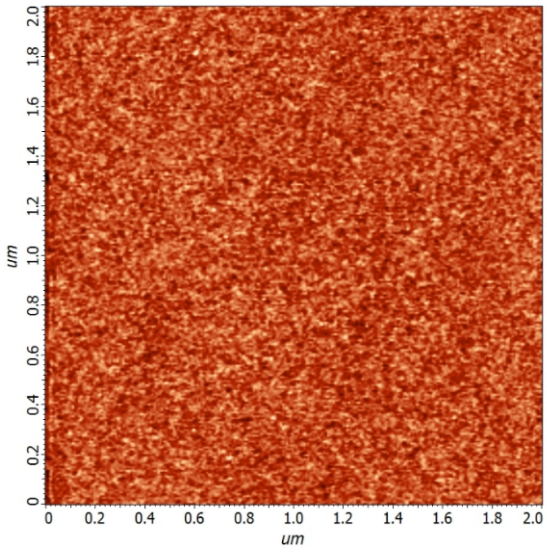

FIGURE 10. 2 μm×2 μm AFM image of the HfZrO thin film.

ACKNOWLDEGMENT

The authors acknowledge also the Technological Department from IMT-Bucharest for their support in manufacturing of the structures.

REFERENCES

[1] T. S. Böscke, J. Müller, D. Bräuhaus, U. Schröder, and U. Böttger, "Ferroelectricity in hafnium oxide thin films," *Appl. Phys. Lett.*, vol. 99, no. 10, Sep. 2011, Art. no. 102903.

[2] J. Müller, T. S. Böscke, U. Schröder, S. Mueller, D. Bräuhaus, U. Böttger, L. Frey, and T. Mikolajick, "Ferroelectricity in simple binary ZrO_2 and HfO_2," *Nano Lett.*, vol. 12, pp. 4318–4323, 2012.

[3] K. Kita, K. Kyuno, and A. Toriumi, "Permittivity increase of yttrium-doped HfO_2 through structural phase transformation," *Appl. Phys. Lett.*, vol. 86, no. 10, Mar. 2005, Art. no. 102906.

[4] M. Modreanu, J. Sancho-Parramon, O. Durand, B. Servet, M. Stchakovsky, C. Eypert, C. Naudin, A. Knowles, F. Bridou, and M.-F. Ravet, "Investigation of thermal annealing effects on microstructural and optical properties of HfO_2 thin films," *Appl. Surf. Sci.*, vol. 253, no. 1, pp. 328–334, Oct. 2006.

[5] P. R. Chalker, M. Werner, S. Romani, R. J. Potter, K. Black, H. C. Aspinall, A. C. Jones, C. Z. Zhao, S. Taylor, and P. N. Heys, "Permittivity enhancement of hafnium dioxide high-*K* films by cerium doping," *Appl. Phys. Lett.*, vol. 93, no. 18, 2008, Art. no. 182911.

[6] Y. Wei, P. Nukala, M. Salverda, S. Matzen, H. J. Zhao, J. Momand, A. S. Everhardt, G. Agnus, G. R. Blake, P. Lecoeur, B. J. Kooi, J. Íñiguez, B. Dkhil, and B. Noheda, "A rhombohedral ferroelectric phase in epitaxially strained $Hf_{0.5}Zr_{0.5}O_2$ thin films," *Nature Mater.*, vol. 17, pp. 1095–1100, Oct. 2018.

[7] S. J. Kim, J. Mohan, S. R. Summerfelt, and J. Kim, "Ferroelectric $Hf_{0.5}Zr_{0.5}O_2$ thin films: A review of recent advances," *JOM*, vol. 71, no. 1, pp. 246–255, Jan. 2019.

[8] T. Shimizu, "Ferroelectricity in HfO_2 and related ferroelectrics," *J. Ceram. Soc. Jpn.*, vol. 126, no. 9, pp. 667–674, Sep. 2018.

[9] M. H. Park, Y. H. Lee, T. Mikolajick, U. Schroeder, and C. S. Hwang, "Review and perspective on ferroelectric HfO2-based thin films for memory applications," *MRS Commun..*, vol. 8, no. 3, pp. 795–808, Aug. 2018.

[10] M. Dragoman, M. Modreanu, I. M. Povey, A. Dinescu, D. Dragoman, A. Di Donato, E. Pavoni, and M. Farina, "Wafer-scale very large memory windows in graphene monolayer/HfZrO ferroelectric capacitors," *Nanotechnology*, vol. 29, no. 42, Aug. 2018, Art. no. 425204.

[11] F. A. McGuire, Y.-C. Lin, K. Price, G. B. Rayner, S. Khandelwal, S. Salahuddin, and A. D. Franklin, "Sustained Sub-60 mV/decade switching via the negative capacitance effect in MoS_2 transistors," *Nano Lett.*, vol. 17, no. 8, pp. 4801–4806, Jul. 2017.

[12] M. Si, C.-J. Su, C. Jiang, N. J. Conrad, H. Zhou, K. D. Maize, G. Qiu, C.-T. Wu, A. Shakouri, M. A. Alam, and P. D. Ye, "Steep-slope hysteresis-free negative capacitance MoS_2 transistors," *Nature Nanotechnol.*, vol. 13, no. 1, pp. 24–28, Dec. 2018.

[13] E. Ko, H. Lee, Y. Goh, S. Jeon, and C. Shin, "Sub-60-mV/decade negative capacitance finfet with sub-10-nm hafnium-based ferroelectric capacitor," *IEEE J. Electron Devices Soc.*, vol. 5, no. 5, pp. 306–309, Sep. 2017.

[14] M. Dragoman, M. Modreanu, I. M. Povey, M. Aldrigo, A. Dinescu, and D. Dragoman, "Electromagnetic energy harvesting based on HfZrO tunneling junctions," *Nanotechnology*, vol. 29, no. 44, Nov. 2018, Art. no. 445203.

[15] M. Dragoman, M. Aldrigo, M. Modreanu, and D. Dragoman, "Extraordinary tunability of high-frequency devices using $Hf_{0.3}Zr_{0.7}O_2$ ferroelectric at very low applied voltages," *Appl. Phys. Lett.*, vol. 110, no. 10, Mar. 2017, Art. no. 103104.

[16] M. Dragoman, M. Modreanu, I. Povey, S. Iordanescu, M. Aldrigo, A. Dinescu, D. Vasilache, and C. Romanitan, "2.55 GHz miniaturised phased antenna array based on 7 nm-thick Hf_x Zr_{1-x} O_2 ferroelectrics," *Electron. Lett.*, vol. 54, no. 8, pp. 469–470, Apr. 2018.

[17] P. Singh and A. K. Verma, "Dielectric loss computation of multilayer Coplanar waveguide," in *Proc. Int. Conf. Commun. Signal Process.*, Feb. 2011, pp. 428–430.

[18] C. Y. Tan, L. Chen, K. B. Chong, and C. K. Ong, "Nondestructive microwave permittivity characterization of ferroelectric thin film using microstrip dual resonator," *Rev. Sci. Instrum.*, vol. 75, no. 1, p. 136, Jan. 2004.

[19] B. Bianco and M. Parodi, "Determination of the propagation constant of uniform microstrip lines," *Alta Freq.*, vol. 45, pp. 107–110, Feb. 1976.

[20] M. Yang, A. KC, A. C. Garcia-Castro, P. Borisov, E. Bousquet, D. Lederman, A. H. Romero, and C. Cen, "Room temperature ferroelectricity in fluoroperovskite thin films," *Sci. Rep.*, vol. 7, p. 7182, Aug. 2017.

[21] A. Ahmed, I. A. Goldthorpe, and A. K. Khandani, "Electrically tunable materials for microwave applications," *Appl. Phys. Rev.*, vol. 2, no. 1, p. 011302, Mar.

[22] Z. Fan, J. Chen, and J. Wang, "Ferroelectric HfO_2-based materials for next-generation ferroelectric memories," *J. Adv. Dielectr.*, vol. 6, Jun. 2016, Art. no. 1630003.

[23] Z. Sun and P. Fay, "Physics-based nonlinear circuit model for coplanar waveguides on silicon substrates," *IEEE Microw. Wireless Compon. Lett.*, vol. 15, no. 10, pp. 709–711, Oct. 2005.

[24] C. Schollhorn, W. Zhao, M. Morschbach, and E. Kasper, "Attenuation mechanisms of aluminum millimeter-wave coplanar waveguides on silicon," *IEEE Trans. Electron Devices*, vol. 50, no. 3, pp. 740–746, Mar. 2003.

[25] M. Dragoman, M. Modreanu, I. Povey, S. Iordanescu, M. Aldrigo, C. Romanitan, D. Vasilache, and D. Dragoman, "Very large phase shift of microwave signals in a 6 nm Hf x Zr1-x O2 ferroelectric at ± 3 V," *Nanotechnology*, vol. 28, no. 38, p. 38, 2017.

[26] R. Simons, *Coplanar Waveguide Circuits, Components, and Systems*. Hoboken, NJ, USA: Wiley, 2001, pp. 15–21.

[27] D. Wang, J. Wang, Q. Li, W. He, M. Guo, A. Zhang, Z. Fan, D. Chen, M. Qin, M. Zeng, X. Gao, G. Zhou, X. Lu, and J. Liu, "Stable ferroelectric properties of $Hf_{0.5}Zr_{0.5}O_2$ thin films within a broad working temperature range," *Jpn. J. Appl. Phys.*, vol. 58, no. 9, Aug. 2019.

[28] M. H. Park, H. J. Kim, Y. J. Kim, Y. H. Lee, T. Moon, K. D. Kim, S. D. Hyun, F. Fengler, U. Schroeder, and C. S. Hwang, "Effect of Zr content on the wake-up effect in $Hf_{1-x}Zr_xO_2$ films," *ACS Appl. Mater. Interfaces*, vol. 8, no. 24, pp. 15466–15475, May 2016.

[29] T. D. Huan, V. Sharma, G. A. Rossetti, Jr., and R. Ramprasad, "Pathways towards ferroelectricity in hafnia," *Phys. Rev. B, Condens. Matter*, vol. 90, no. 6, Jul. 2014, Art. no. 064111,

[30] D. M. Hausmann and R. G. Gordon, "Surface morphology and crystallinity control in the atomic layer deposition (ALD) of hafnium and zirconium oxide thin films," *J. Cryst. Growth*, vol. 249, nos. 1–2, pp. 251–261, Feb. 2003.